



2003

The Photochemistry of Nitrous Acid in an Aqueous Matrix

Jay S. Ratliff '03

Illinois Wesleyan University

Follow this and additional works at: https://digitalcommons.iwu.edu/chem_honproj

 Part of the [Chemistry Commons](#)

Recommended Citation

Ratliff '03, Jay S., "The Photochemistry of Nitrous Acid in an Aqueous Matrix" (2003).
Honors Projects. 3.

https://digitalcommons.iwu.edu/chem_honproj/3

This Article is protected by copyright and/or related rights. It has been brought to you by Digital Commons @ IWU with permission from the rights-holder(s). You are free to use this material in any way that is permitted by the copyright and related rights legislation that applies to your use. For other uses you need to obtain permission from the rights-holder(s) directly, unless additional rights are indicated by a Creative Commons license in the record and/ or on the work itself. This material has been accepted for inclusion by faculty at Illinois Wesleyan University. For more information, please contact digitalcommons@iwu.edu.

©Copyright is owned by the author of this document.

The Photochemistry of Nitrous Acid in an Aqueous Matrix

Jay Ratliff

Chemistry 499, 2002-2003

Senior Research Honors Thesis

Abstract:

The thermal and photochemical decomposition of aqueous solutions of nitrous acid and nitrite ion were studied, with a focus on the production and subsequent reaction of hydroxyl radicals. The production of these radicals in aqueous solution may be determined indirectly by disappearance of nitrous acid, or more directly by their interaction with a radical scavenger. Benzene was used to scavenge hydroxyl radical and the products of reactions with hydroxyl radical as well as nitrous acid were characterized. The roles of temperature and dissolved gases were also examined.

Theory:

The atmosphere, which is a mixture of different gases, particles, and aerosols, is very important to sustaining life. The atmosphere protects life by filtering out cosmic rays, ultraviolet radiation, and even meteors, thus preventing them from reaching the surface. The atmospheric pressure, and thus density of the air, decreases with increasing altitude. Half of the mass of the atmosphere¹ is in the lowest 5 km, while 99% of the mass is below about 25 to 30 km. The atmosphere has a number of layers, including the troposphere, tropopause, and stratosphere (see Figure 1). The lowest layer, the troposphere, ranges in height from 8 km near the poles to 16 km near the equator¹. The troposphere is bounded above by the tropopause, which is a region of stable temperature. The troposphere also contains nearly all of the atmospheric water vapor¹. The temperature in the troposphere usually decreases with increasing altitude¹. As the temperature decreases, the density of the air increases. Thus, the troposphere mixes vertically. This vertical mixing of air causes most of the world's weather. Above the tropopause is the stratosphere, which contains the ozone layer. This ozone layer is responsible for filtering out most of the harmful ultraviolet light from the sun. The temperature in the stratosphere usually increases with increasing altitude, which prevents much mixing between the troposphere and stratosphere.

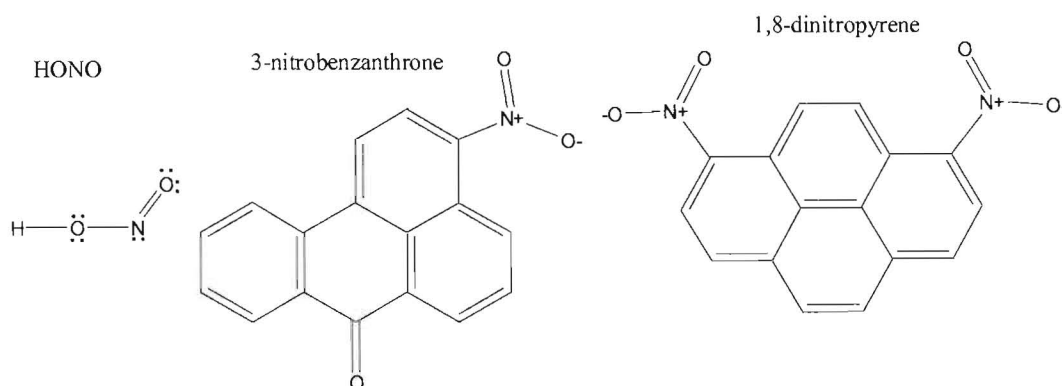
Sometimes the temperature in the troposphere increases with altitude instead of decreasing; this is called a temperature inversion. In a temperature inversion the temperature driven mixing of air is absent and thus the air does not mix vertically. This causes pollution emitted at ground level to be trapped underneath the temperature inversion¹. Long known for its foggy weather and coal-burning homes, power plants, and factories, London, England, experienced dense smog from December 5th to December 9th, 1952. According to official government reports, this lethal fog resulted in about 3,000 more deaths² than normal during the first 3 weeks of December 1952. Since the death rate was more than 3 times the average for this period, the London fog of 1952 is widely regarded as a catalyst for the study of air pollution epidemiology².

Aerosols are solid or liquid particles dispersed in the air, and include dust, soot, sea salt crystals, spores, bacteria, viruses, and many other microscopic particles¹. Aerosols typically have diameters in the region of 0.001 to 10 μm . Primary aerosols are formed by the dispersal of material at the surface, whereas secondary aerosols are formed by reaction of gases in the

atmosphere. Primary aerosols include volcanic dust, organic materials from biomass burning, soot from combustion, and mineral dust from wind-blown processes, while secondary aerosols include sulfates from the oxidation of sulfur-containing gases during the burning of fossil fuels, nitrates from gaseous nitrogen species, and products from the oxidation of volatile organic compounds¹.

Aerosols also can act as sites for heterogeneous chemical reactions to take place³. The most significant of these reactions are those that lead to the destruction of stratospheric ozone. During winter in the polar regions, aerosols grow to form polar stratospheric clouds³. The large surface areas of these cloud particles provide sites for chemical reactions to take place. These reactions lead to the formation of large amounts of reactive chlorine and, ultimately, to the destruction of ozone in the stratosphere. Evidence now exists that shows similar changes in stratospheric ozone concentrations occur after major volcanic eruptions, like Mt. Pinatubo in 1991, where tons of volcanic aerosols are blown into the atmosphere³.

Figure 2: Nitrous Acid (HONO), 3-Nitrobenzanthrone, and 1,8-Dinitropyrene

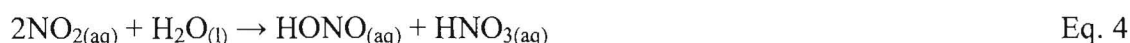


Nitrous acid (see Figure 2) has the formula HONO and is an important factor in the environment due to its role in the chemistry of the troposphere, but its behavior in the environment is not well understood. Polluted air masses are typically characterized by high concentrations of oxidized nitrogen compounds⁴. Nitrogen oxides not only ultimately form nitric acid, the major component of acid rain, which corrodes statues and buildings, damages crops and forests, and makes lakes and streams unsuitable for fish and other plant and animal life, they also play important roles in the formation of secondary photooxidants, such as ozone, hydroxyl radical, and hydrogen peroxide, that control the oxidation of sulfur dioxide and other species such as hydrocarbons⁵. Toxic nitroderivatives such as 3-nitrobenzanthrone and 1,8-dinitropyrene are the most powerful direct mutagens thus far detected in atmospheric particulates⁶. Oxidized

nitrogen compounds are commonly emitted from internal combustion engines. At the high temperatures of internal combustion engines, nitrogen and oxygen react to form nitric oxide (NO). NO then reacts with additional oxygen to form nitrogen dioxide (NO₂):



Commonly, NO and NO₂ are collectively referred to as NO_x. It has been proposed⁵ that NO and NO₂ react with liquid water to form nitrous acid and nitric acid (HNO₃). The subsequent liberation of HONO to the gas phase is a major source of HONO in the gas phase⁵.



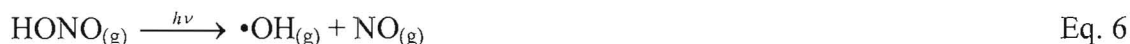
It has been shown that aqueous phase formation of HONO cannot account for the concentrations observed in the troposphere^{7,8}. As a result, heterogeneous formation of HONO has been proposed through both solid surface catalyzed reactions^{4,9,10} and aerosol reactions involving NO, NO₂, H₂O, and aerosols¹¹.



In this reaction, the soot substrate is oxidized, while the NO₂ is reduced. The reducing groups are believed to be C-O and C-H groups in the soot. The study found HONO production to be steady over a humidity range from 0.5% to 60%.

HONO has been shown to increase in concentration during the night and decrease in concentration rapidly upon dawn^{12,13,14,15}. A HONO concentration of 8 ppbv has been observed in the gas phase¹³ and natural dew waters in Hiroshima, Japan were found⁸ to have concentrations of N(III) between 2.3 and 17.4 μM, where N(III) is the total concentration of HONO and its conjugate base NO₂⁻. Nitrous acid and nitrite ion both absorb light between 300 and 400 nm (see Figure 6). The overall shape of the peak for both HONO and NO₂⁻ is due to a *n* to *π*^{*} electronic transition. The fingertips on the HONO spectrum are due to different vibrational transitions. This absorbance is important because ultraviolet light of shorter wavelengths is absorbed by ozone (see Figure 3). Wavelengths between 300 and 400 nm correspond to about 400 to 300 kJ/mol. Thus, wavelengths longer than 400 nm are too low in energy to overcome the bond energies of most atmospheric compounds, while wavelengths shorter than 300 nm are absorbed by the upper atmosphere and do not reach the troposphere (see Figures 4 and 5).

At dawn, HONO is photolyzed following absorption of 300-400 nm light¹⁶ to form hydroxyl radicals ($\bullet\text{OH}$) and nitric oxide according to the following reaction¹⁷:



In the absence of a scavenger, hydroxyl radicals and nitric oxide will likely recombine to form HONO. However, atmospheric oxygen will scavenge nitric oxide while NO_2 will scavenge hydroxyl radicals^{18, 16}:



NO_2 will also undergo photolysis at wavelengths shorter than 410 nm to form $\bullet\text{O}$. The $\bullet\text{O}$ then reacts with atmospheric oxygen to form ozone.



Ozone is beneficial in the stratosphere because it prevents ultraviolet radiation from striking the earth, but in the troposphere its strong oxidizing properties cause harmful reactions. Ozone concentration in remote areas ranges from 20 to 50 ppb, whereas in urban centers it ranges from 100 to 500 ppb¹⁹. At a concentration of about 100 ppb ozone becomes toxic to plants and animals due to a high reactivity of ozone compared to oxygen.

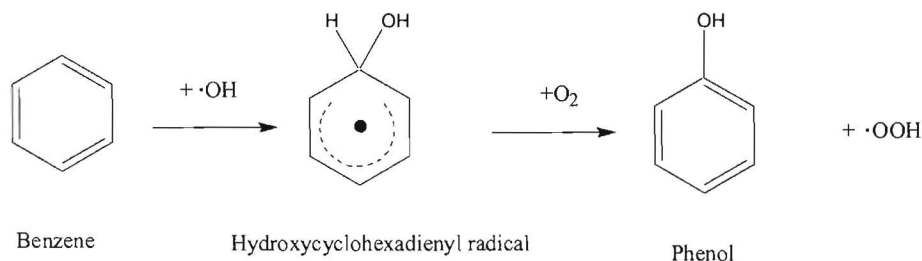
The hydroxyl radical is very reactive and the most aggressive naturally occurring oxidant in the environment²⁰. The lifetimes of many compounds in the troposphere are determined by oxidation reactions with hydroxyl radicals. HONO is a significant source of hydroxyl radicals for the first few hours after dawn⁸. Photochemical smog, first discovered in Los Angeles in the 1940s, is largely composed of products of reactions of hydroxyl radicals with volatile organic compounds released by factories and other pollution sources. Hydroxyl radicals are difficult to monitor directly because they are unstable in solution and absorb below 200nm. Thus, they cannot be monitored by conventional ultraviolet-visible spectroscopy (UV-VIS). To track production of $\bullet\text{OH}$, it must be scavenged and the products of the scavenging reaction monitored.

Environmental chemistry is very complex due to the interactions between competing reactions. The atmospheric variability in terms of temperature, radiation flux, suspended aerosols, particulates, and differences due to geography or local anthropogenic emissions makes the study of atmospheric reactions difficult. There is evidence⁵ that aqueous phase reactions (such as those occurring in aerosols) contribute significantly to the concentration of HONO in

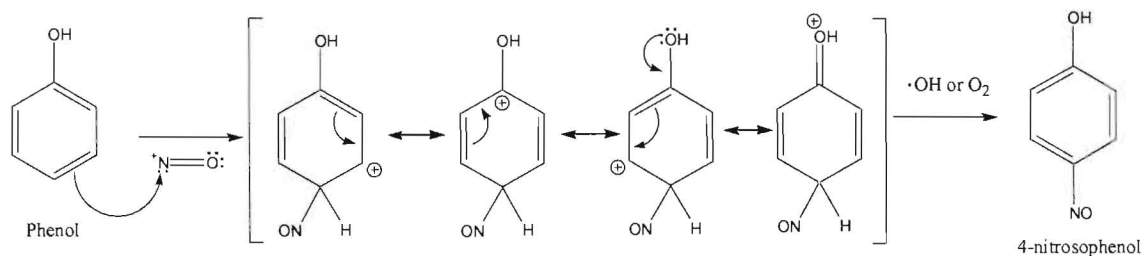
the gas phase, and thus there must be HONO in atmospheric aerosols. Aerosols provide an aqueous environment that is rich in organic matter. Since many aerosols have a solid core, there could also be heterogeneous surface reactions involving HONO. A majority of the earth is covered with water, either freshwater or saltwater, and thus there may be significant amounts of N(III) compounds involved in aqueous reactions important in environmental chemistry.

To model the study of HONO aerosol photolysis, the aqueous phase reactions of HONO will be studied. The aqueous phase, however, presents additional concerns, such as cage effects. In condensed phases the solute molecule is surrounded by solvent atoms or molecules. This "cage" exerts forces directed against the escape of the reaction products. Thus, when HONO undergoes photolysis to NO and $\bullet\text{OH}$, the water molecules will tend to prevent the NO and $\bullet\text{OH}$ from migrating and thus reacting with other species in solution. As a result, the recombination of NO and $\bullet\text{OH}$ becomes more likely and decreases the quantum yield of HONO disappearance.

Hydroxyl radicals in aqueous solution react with benzene to form phenol¹⁶ with a rate constant of $7.8 \times 10^9 \text{ Lmol}^{-1}\text{s}^{-1}$. The yield of phenol from the reaction of benzene with hydroxyl radical was determined²¹ as $\alpha = 0.95 \pm 0.1$. Phenol subsequently undergoes a thermal reaction with HONO to form p-nitrosophenol:



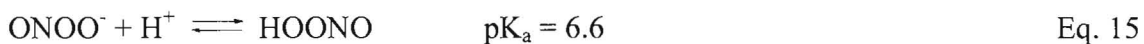
Eq. 11



Eq. 12

In aqueous solution containing dissolved nitric oxide, $\bullet\text{OOH}$ found in Eq. 11 is expected to form mainly peroxynitrous acid¹⁶ (HOONO).





Peroxynitrous acid can then decompose¹⁶ into nitric acid or •OH and NO₂:



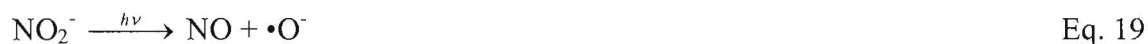
Solutions of N(III) and benzene (at pH= 2.0 and 5.6) kept in the dark did not form any detectable phenol over 1 hour, thus any phenol formed during a photolysis trial is not due to thermal reactions between N(III) and benzene⁸.

The measured extinction coefficients for aqueous HONO at 357 and 371 nm are 4.07 and 4.26 m² mol⁻¹ respectively¹⁶. The reported quantum yield of hydroxyl radical ($\Phi_{\bullet\text{OH}}$) for the photolysis of nitrous acid was constant at 0.35 for the wavelength range from 280 nm to 390 nm, whereas the reported $\Phi_{\bullet\text{OH}}$ for the photolysis of nitrite ion (NO₂⁻) was about five times less over the same wavelength range¹⁶. Similarly, hydroxyl radical photoformation rates were found⁸ to be higher at lower pH values and were linearly dependent on the concentration of N(III). Thus nitrous acid is a much more efficient source of hydroxyl radicals than the nitrite ion.

In aqueous solution, HONO undergoes acid-base dissociation⁵ with a pK_a of 3.27:



Nitrite ion undergoes a photolysis reaction following absorption of 300-400 nm light¹⁶ to form nitric oxide and hydroxyl radicals^{22, 16}:



Nitrite can also act as a sink for hydroxyl radicals at a diffusion-controlled rate²² to form NO₂:



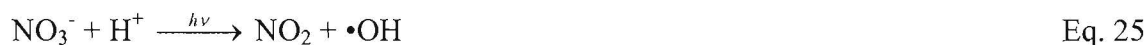
Nitrogen dioxide has been shown²² to promote the nitration of a variety of organic compounds such as phenol^{23, 24, 25, 26, 27} and various azaarenes²⁸ that can be nitrated directly by NO₂, while the nitration of benzene²⁹ is assisted by •OH. However, the above reaction only becomes significant if the nitrite concentration is considerably higher than the usual nitrite concentration in the environment and thus the nitration of phenol and various azaarenes upon nitrite photolysis is possible only at high nitrite concentration (up to 0.1 M)²². It has been shown that certain compounds including TiO₂ in aqueous suspension and Fe(III) in aqueous solution enhance phenol photonitration in the presence of nitrite²². The TiO₂ enhancement involves

adsorbed hydroxyl radicals and the Fe(III) involves an increase in hydroxyl radical production in solution. The additional hydroxyl radical reacts with HONO and nitrite ion to form NO₂, which then reacts with phenol. Thus, the generation of NO₂ can be significant at lower concentrations of HONO and NO₂⁻ than in nitrite photolysis alone.

Phenol nitration in the presence of nitrite at pH 1.5 is due²² to thermal processes involving HONO and possibly to the nitrous acid thermal decomposition to NO and NO₂ as well as the photolysis of HONO:



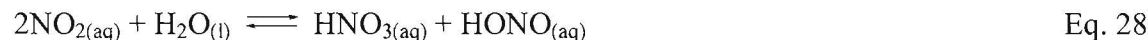
Nitrate also undergoes a photolysis reaction at wavelengths shorter than 350 nm (see Figure 7) to form NO₂ and •OH. The •OH can then oxidize nitrite to nitrogen dioxide, further enhancing phenol nitration²².



Nitrous acid in aqueous solution thermally decomposes as follows. The decomposition was found to be first order at low concentration, and the rate is affected by temperature and ionic strength³⁰.



Park and Lee propose a reversible decomposition of HONO to NO and NO₂. The NO₂ produced undergoes hydrolysis to yield nitric and nitrous acids⁵:



Nitrous acid is also in equilibrium with its anhydride, N₂O₃, which can dissociate into NO and NO₂:



Previous findings³¹ suggest that the mechanism of aromatic nitration in aqueous nitric acid proceeds as follows:



Encounter pair \rightarrow Conjugated carbocation intermediate \rightarrow Product Eq. 34

Phenol, 4-nitrosophenol, and nitrate were previously¹⁶ observed as HONO photolysis products in the presence of benzene. The fraction of the concentration of nitrosophenol to that of phenol rose linearly with time to 5.5% after 1h, which indicates that nitrosophenol is a secondary product. Phenol is known^{32, 33} to react thermally with HONO to give a 95% yield of 4-nitrosophenol. The nitrosating agent is known³⁴ to be N_2O_3 .

In this study, the thermal and photochemical decomposition of aqueous solutions of nitrous acid and nitrite ion will be studied. The major focus will be on the production and subsequent reaction of hydroxyl radicals. The production of these radicals in aqueous solution may be determined indirectly by disappearance of nitrous acid, or more directly by their interaction with a radical scavenger. The mechanism of scavenging reactions that trap the hydroxyl radical will be studied, and characterization of the products of these reactions will be attempted.

Experimental:

Solutions of 0.050M nitrous acid were prepared by adding 10.0 mL of 0.50 M NaNO_2 (Baker and Adamson, reagent grade, MW 68.99527 g/mol) to 10.0 mL of 0.25 M H_2SO_4 (Fisher Scientific, reagent grade, MW 98.0734 g/mol) and diluting the resulting solution to 100.0 mL with house reverse osmosis deionized water in a volumetric flask. Solutions for controlled temperature experiments were prepared as above with component solutions pre-chilled in an ice bath. Benzene (Fisher Scientific, reagent grade, 99.9%, MW 78.1134 g/mol) saturated solutions of nitrous acid were prepared by shaking solutions of 0.050M nitrous acid with benzene and then separating the aqueous layer from the organic layer. Approximately 80 mL of the prepared solution were placed in a quartz tube for reaction.

Photolysis of solutions was conducted in a Rayonet Photochemical Reactor, Model RPR-100. Solutions were irradiated at approximately 366 nm using Rayonet Photochemical Reactor Lamps, Model RPR-3500A, for 60 minutes unless stated otherwise. A Precision Scientific Group chiller, Model 66459, was utilized to control the temperature of the solutions during photolysis. Photolysis of solutions was conducted with the chiller set to -2°C unless stated otherwise. The actual temperature of the solution was approximately 5°C .

Thermolysis of solutions was conducted in the photoreactor with the lamps off to obtain reaction conditions similar to photolysis reactions. Thermolysis reactions were conducted for 60 minutes with the chiller set to 0°C unless stated otherwise. The actual temperature of the solution was approximately 5°C .

Ultraviolet-Visible (UV-VIS) spectra were determined using a Varian Cary 1 UV-VIS spectrometer using quartz cells of 1.0 cm path length and reference solutions of 0.025 M Na_2SO_4 (Aldrich, reagent grade, MW 142.03714 g/mol) or 0.025 M Na_2SO_4 saturated with benzene. UV-VIS spectra were determined for standard aqueous solutions of HONO , NaNO_2 , HNO_3 (Fisher Scientific, reagent grade, MW 63.0128 g/mol), and benzene.

Solutions to be analyzed by Gas Chromatography-Mass Spectrometry (GC-MS) were placed in a large beaker and a stream of air was blown across the surface of the solution to evaporate the water. After approximately 24 hours, the water and excess benzene had evaporated, leaving dark brown crystals. Ethanol (AAPER Alcohol and Chemical, reagent grade, 200 proof, MW 46.0688 g/mol) was added to dissolve the organic products while leaving the insoluble sodium sulfate salt behind. Samples of 2 μL of the ethanol solution were analyzed

by GC-MS. GC-MS was performed on an HP 6890 GC-MS with an HP-5 crosslinked 5% phenyl methyl siloxane column (30 m long, 32 mm inner diameter, 0.25 μ m thick film, phase ratio = 320) and the peaks were identified by comparison to the internal library of compounds as well as standards run under similar conditions. Standards included ethanol, benzene, 4-aminophenol (Aldrich, reagent grade, 99%, MW 109.13 g/mol), 2-aminophenol (Aldrich, reagent grade, 99%, MW 109.13 g/mol), 2-nitrophenol (Eastman Organic Chemicals, reagent grade, MW 139.1104 g/mol), 3-nitrophenol (Acros, reagent grade, 99%, MW 139.1104 g/mol), 4-nitrophenol (Aldrich, reagent grade, MW 139.1104 g/mol), 1,4-benzoquinone (Fisher Scientific, reagent grade, MW 108.0964 g/mol), 4-nitrosophenol (Aldrich, reagent grade, MW 123.111 g/mol), phenol (Aldrich, reagent grade, MW 94.1128 g/mol), and nitrobenzene (Eastman Organic Chemicals, reagent grade, MW 123.111 g/mol).

An infrared (IR) spectrum of the dried photolysate in a KBr pellet was recorded on a Mattson Genesis Series FT-IR Model 9423.

Thin Layer Chromatography (TLC) was performed on the dried photolysis product using a 1:1 mixture of methanol and benzene and silica gel plates.

Results and Discussion:

Characterization of reactants

The UV-VIS spectrum of HONO in aqueous solution shows a characteristic “handprint” with five local maxima at 335, 346, 358, 371, and 385 nm (± 1 nm) with molar absorptivities of 2.24, 3.60, 4.80, 4.60, and $2.96 \text{ m}^2\text{mol}^{-1}$ respectively. These values compare favorably with those of Fischer and Warneck¹⁶. The UV-VIS spectrum of sodium nitrite in aqueous solution has a single broad maximum at 355 nm (± 1 nm) with a molar absorptivity of $2.36 \text{ m}^2\text{mol}^{-1}$. The UV-VIS spectrum of benzene in aqueous solution has six local maxima at 208, 238, 243, 248, 253, and 259 nm (± 1 nm).

The thermal decomposition of HONO

The nitrous acid solution decomposes in the thermal reaction that forms NO and HNO₃. See Table 1 for the percent decomposition during photolysis and thermolysis of HONO solutions and benzene saturated (0.18 g/100 mL at 25°C)³⁵ HONO solutions. As the temperature decreases the thermal decomposition of HONO decreases. The decomposition of HONO during the photolysis reactions was higher than similar temperature thermolysis reactions. This difference may be partly due to an increase in temperature due to the energy input from the light, but HONO has a self-scavenging mechanism that produces NO and NO₂ as follows:



However, when benzene is present to scavenge hydroxyl radical produced in the photolysis of HONO, the depletion of HONO is significantly greater.

Table 1: Analysis of Thermal and Photochemical Decomposition of HONO by UV-VIS

Run Type	Temp of Chiller (°C) *	Avg. of % Change @60min **	Std. Dev
Photo HONO	5.0	5.32	0.67
Thermo HONO	5.0	4.05	0.57
Photo HONO	-2.0	1.86	0.33
Thermo HONO	-2.0	1.34	0.51
Thermo HONO, Ben	-2.0	0.29	0.43
Thermo HONO, Ben	0.0	3.22	0.47
Photo HONO, Ben	-2.0	77	5.3

* The solution temperature was approximately 2°C higher for the thermolysis reactions and 4°C higher for the photolysis reactions.

** The average of the decrease in absorbance values of the five peaks of the HONO handprint

The photochemical decomposition of HONO

The benzene saturated HONO solution was colorless but turned a dark brown during photolysis. After drying, the residue remaining was a brown, crystalline solid. Upon washing with ethanol, the ethanol dissolved the dark brown product but left behind a white, crystalline solid. This solid should be sodium sulfate, which is insoluble³⁶ in ethanol, but was not analyzed. The dark brown ethanol solution was analyzed using GC-MS. Three of the four product peaks were identified to be phenol, 4-nitrosophenol, and 4-nitrophenol using the library of compounds as well as comparison to standards run under the same chromatographic conditions. The ratio of 4-nitrosophenol to 4-nitrophenol was approximately 15:1. The phenol peak was difficult to quantify because it is situated on the tail of the solvent peak. The fourth product peak is believed to be benzoquinone or aminophenol. Attempts to add the products from multiple photolysis reactions together to have more of the minor product for GC-MS analysis were unsuccessful.

An IR spectrum of the photolysis product was determined to identify the minor photolysis product. See Table 2 for expected IR stretches. No amine peak was detected, which indicates that the minor product is not aminophenol. However, no C=O peak was detected, which indicates that the minor product is not benzoquinone. However, the spectrum quality is not high, largely due to low transmittance values. The low transmittance occurred because the pellet was too thick and absorbed too much of the incident IR radiation. Numerous attempts

were made to obtain a better quality spectrum, but efforts were hampered by the inability to obtain an unbroken KBr pellet that was thin enough. Another possible reason that neither of the expected peaks appeared is that the minor product was present in such low quantities because the ratio of the minor product to 4-nitrosophenol was very low. As a result, the IR peaks due to the minor product would be much smaller than the peaks due to 4-nitrosophenol and would likely not be observed. TLC of the photolysis product was unsuccessful in separating the component compounds and thus retention factors were not calculated.

Table 2: Expected IR Stretches³⁷

Bond	Specific Context	Product associated with stretch	Frequency (cm ⁻¹)
O-H	ROH	Phenol, nitrosophenol, nitrophenol, aminophenol	3200-3400
N-O	RNO ₂	Nitrophenol	1350,1560
N-O	RN=O	Nitrosophenol	1500-1600
Aromatic	Mono-substituted	Phenol	730-770, 690-710 (two)
	Para-substituted	Nitrosophenol, nitrophenol, aminophenol, benzoquinone	810-840
C=O	Ar-C=O	Benzoquinone	1690
N-H	RNH ₂	Aminophenol	3400-3500 (two)

The effect of dissolved gases on product abundance

To determine the effect of dissolved gases upon product abundance, solutions for photolysis were purged with O₂ or N₂. The product abundance of photolysis of solutions purged with either O₂ or N₂ did not change significantly from photolysis of solutions open to air. This indicates that the 4-nitrophenol is not created by the oxidation of 4-nitrosophenol by dissolved oxygen. Attempts to dry the photolysis solution under an atmosphere of nitrogen instead of air were unsuccessful.

The effect of time on product abundance

To examine the possibility of a thermal oxidation process converting 4-nitrosophenol to 4-nitrophenol in solution, a photolysis reaction was performed and the resulting solution was

allowed to stand open to the atmosphere at room temperature for 24 hours prior to drying. The product abundances changed significantly. The ratio of 4-nitrosophenol to 4-nitrophenol was approximately 1:1. However, it is difficult to determine whether or not the quantity of 4-nitrosophenol decreased while the quantity of 4-nitrophenol increased. The abundance of each product as determined by the GC was not reproducible. This could be due to differing concentrations of product in the ethanol solution due to differences in the volume of ethanol used to dissolve the organic products. A decrease in the quantity of 4-nitrosophenol would be consistent with an oxidation process reacting 4-nitrosophenol to 4-nitrophenol. However, if the quantity of 4-nitrosophenol did not decrease, a direct nitration of phenol becomes more likely.

Photolysis product mass

The mass of solid product of the photolysis of 80 mL of 0.05 M HONO saturated with benzene (after evaporation of water) was 0.3456 g. The solid was then washed with ethanol to dissolve the organic products. The mass remaining was 0.2922 g, which is slightly greater than the theoretical mass of Na_2SO_4 that should remain (0.2841 g). The calculated mass of product that dissolved in the ethanol was 0.0534 g. Theoretical masses of reactants in 80 mL of a benzene saturated 0.05 M HONO solution and the experimental masses of the dried products is presented in Table 3.

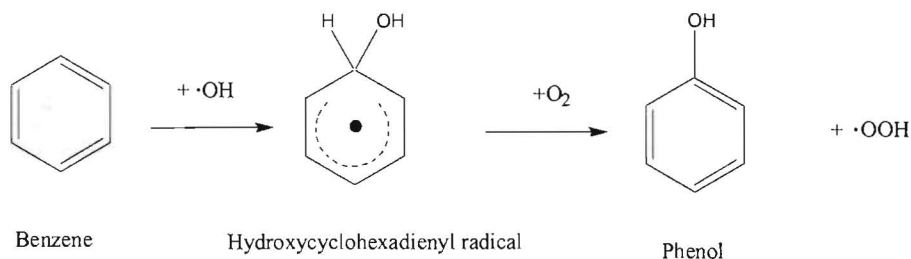
Table 3: Theoretical and Experimental Masses of Reactants and Products in 80mL of Benzene Saturated HONO Photolysis Solution

Quantity	Mass (g)
Theoretical mass of benzene	0.144
Theoretical mass of HONO	0.188
Theoretical mass of Na_2SO_4	0.2841
Total solid product after drying	0.3456
Solid product remaining after ethanol washing	0.2922
Calculated mass of product in ethanol solution	0.0534

Proposed reaction schemes

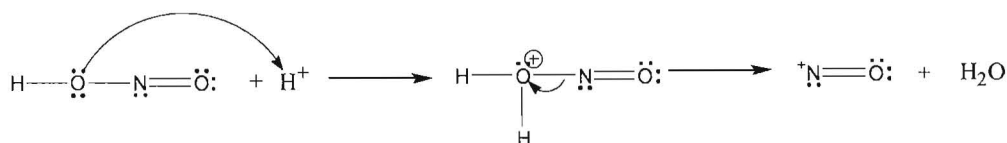
Benzene is known to react with hydroxyl radical to form phenol proceeding via the hydroxycyclohexadienyl radical as in Scheme 1.

Scheme 1

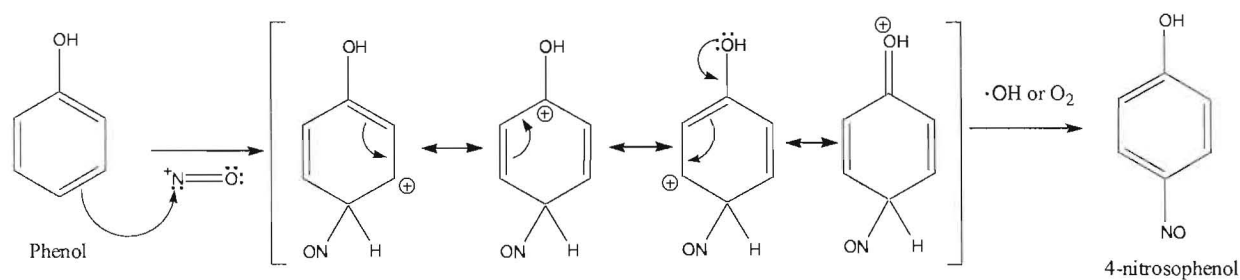


Phenol can then react with NO^+ formed from HONO as in Scheme 2 to form 4-nitrosophenol in an electrophilic aromatic substitution as in Scheme 3. The NO^+ is directed to the para- position by the ortho-/para- activating OH group.

Scheme 2

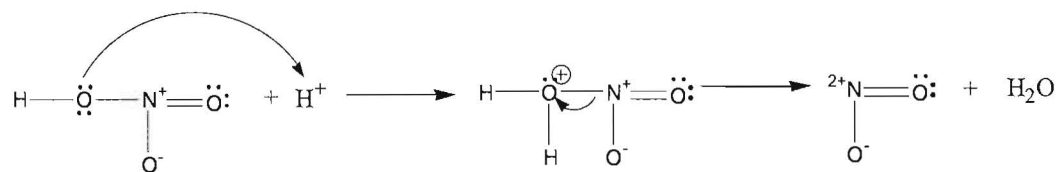


Scheme 3

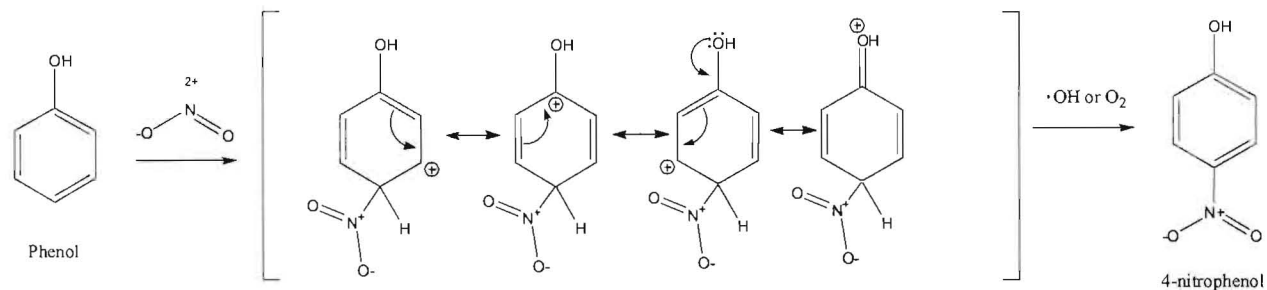


Phenol can also react with NO_2^+ formed from HNO_3 as in Scheme 4 to form 4-nitrophenol in an electrophilic aromatic substitution as in Scheme 5. Again, the NO_2^+ is directed to the para- position by the ortho-/para- activating OH group.

Scheme 4

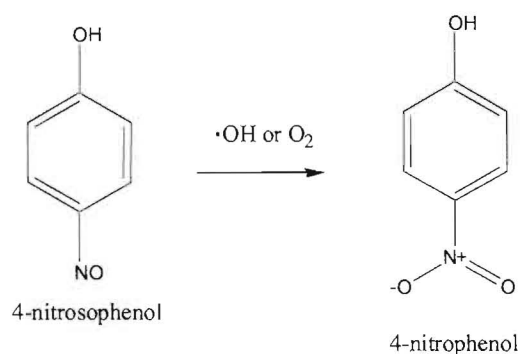


Scheme 5



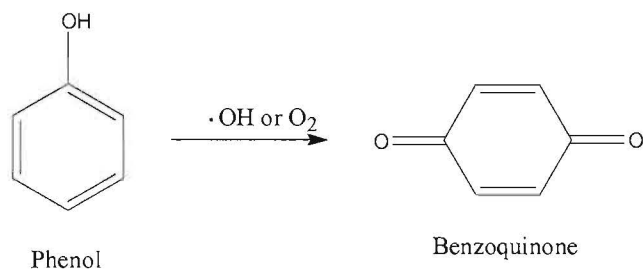
4-Nitrophenol might also be produced in an oxidation reaction involving 4-nitrosophenol as in Scheme 6.

Scheme 6

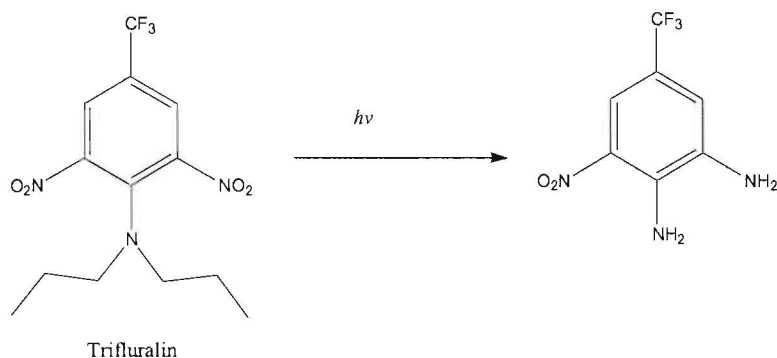


The minor photolysis product that has been tentatively identified as either benzoquinone or aminophenol could be synthesized in two ways. Phenol could be oxidized to form benzoquinone as in Scheme 7. Nitro-aromatics are known to reduce to amines under reducing conditions, such as a H_2 bubbled solution in the presence of a Pd catalyst. Mongar and Miller³⁸ have shown that trifluralin is photoreduced to an amine as in Scheme 8.

Scheme 7

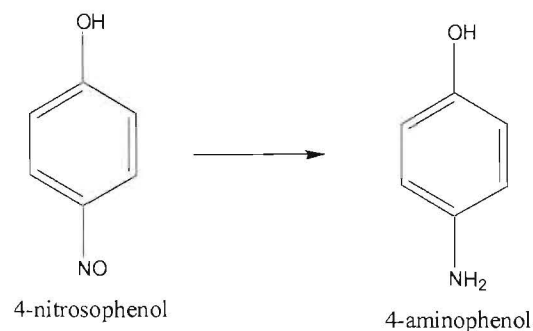


Scheme 8



Nitrosophenol is reduced from nitrophenol and the reduction of nitrosophenol to aminophenol should be favored over the reduction of nitrophenol to aminophenol, as in Scheme 9. However, reducing conditions are not likely to have occurred, since a major product is 4-nitrophenol and thus may have been oxidized from 4-nitrosophenol. Nitrosophenol is unlikely to be reduced to one product and oxidized to another under the same reaction conditions. This favors the hypothesis that benzoquinone is the minor photolysis product.

Scheme 9



Conclusions:

The thermal and photochemical decomposition of aqueous solutions of nitrous acid and nitrite ion were studied, with a focus on the production and subsequent reaction of hydroxyl radicals. The production of these radicals in aqueous solution may be determined indirectly by disappearance of nitrous acid, or more directly by their interaction with a radical scavenger. Benzene was used to scavenge hydroxyl radical and the products of reactions with hydroxyl radical as well as nitrous acid were characterized. The role of temperature and dissolved gases were also examined.

The thermal decomposition of HONO to NO and HNO₃ was found to decrease as temperature decreased. The UV-VIS spectrum of HONO indicates a 3% decrease in absorbance after 60 minutes of thermal decomposition in the presence of benzene, as compared to a 77% decrease in absorbance after 60 minutes of irradiation using approximately 366 nm light in the presence of benzene.

The major products of a 1-hour photolysis of a benzene saturated aqueous solution of nitrous acid were identified as phenol, 4-nitrosophenol, and 4-nitrophenol. A minor product was tentatively identified as either 1,4-benzoquinone or 4-aminophenol. The 4-nitrophenol was found to be produced in a thermal reaction. The mechanism for 4-nitrophenol formation is unclear, as it could be direct nitration of phenol or oxidation of 4-nitrosophenol. Dissolved N₂ and O₂ did not affect product abundance.

Future Work:

Further work can be done to investigate the pH dependence of the photolysis of the nitrous acid/nitrite system. Isolation, identification, and quantification of all products, but especially the minor photolysis product, would also be beneficial. Further attempts could be made to conduct a photolysis under N₂ and dry the products under N₂ to prevent oxidation of 4-nitrosophenol to 4-nitrophenol. Future work could also focus on any temperature dependence of the product abundance of the photolysis of HONO using a benzene scavenger. Another scavenger could be used to scavenge hydroxyl radical. Alcohols may be used as scavengers to investigate the photolysis, since they have successfully been used to scavenge hydroxyl radical in the past²².

Acknowledgements:

The author would like to thank Dr. Timothy Rettich for his overall support and understanding, Dr. Rebecca Roesner and Dr. Jeff Frick for chromatographic assistance, Cindy Honneger for her assistance with equipment and materials, Dr. Stephen Hoffmann for helpful conversations, and the rest of the Illinois Wesleyan University Chemistry Department.

References:

1. "Atmosphere", <http://www.doc.mmu.ac.uk/aric/eae/Atmosphere/atmosphere.html>.
2. Bell, M.; Davis, D. L.; *Environ. Health Persp.* (2001) **109**.
3. "Atmospheric Aerosols: What Are They, and Why Are They So Important?"
<http://oea.larc.nasa.gov/PAIS/Aerosols.html>
4. Ammann, M.; Kalberer, M.; et al. *Nature*, (1998), **395**, 157.
5. Park, J.; Lee, T. *J. Phys. Chem.*, (1988), **92**, 6294.
6. Enya, T.; Suzuki, H.; Watanabe, T.; Hirayama, T.; Himasatsu, Y. *Environ. Sci. Technol.*, (1997), **31**, 2772.
7. Lammel, G.; Cape, J.N. *Chem. Soc. Rev.*, (1996), 361.
8. Arakaki, T.; Miyake, T.; Hirakawa, T.; Sakugawa, H. *Environ. Sci. Technol.*, (1999), **33**, 2561.
9. Sakamaki, F.; Hatakeyama, S.; Akimoto, H. *Int. J. Chem. Kinet.*, (1983), **15**, 1013.
10. Jenkin, M. E.; Cox, R. A.; Williams, D. J. *Atmos. Environ.*, (1988), **22**, 487.
11. Notholt, J.; Hjorth, J.; Raes, F. *Atmos. Environ.*, (1992), **26A**, 211.
12. Perner, D.; Platt, U. *Geophys. Res. Lett.*, (1979), **6**, 917.
13. Harris, G. W.; Carter, W. P. L.; Winer, A. M.; Pitts, J. N.; Platt, U.; Perner, D. *Environ. Sci. Technol.*, (1982), **16**, 414.
14. Pitts, J. N.; Biermann, H. W.; Atkinson, R.; Winer, A. M. *Geophys. Res. Lett.*, (1984), **11**, 557.
15. Sjödin, A.; Ferm, M. *Atmos. Environ.*, (1985), **19**, 985.
16. Fischer, M.; Warneck, P. *J. Phys. Chem.*, (1996), **100**, 18749.
17. Cox, R.A.; Atkins, D.H. *U.K. At. Energy Res. Estab. Rep.*, (1973) AER-R7615.
18. Finlayson-Pitts, B.J.; Pitts, J.N. *Science*, (1997), **278**, 1776.
19. "Ground Level Ozone", <http://www.maineskeptic.com/groundlevelozone.html>.
20. Bilski, P.; Chignell, C.F.; et al. *J. Am. Chem. Soc.*, (1992), **114**, 549.
21. Deister, U.; Warneck, P.; Wurzinger, C. *Ber. Bunsen-Ges. Phys. Chem.*, (1990), **94**, 594.
22. Vione, D.; Maurino, V.; Minero, C.; Pelizzetti, E. *Environ. Sci. Technol.*, (2002), **36**, 669.
23. Machado, F.; Boule, P. *J. Photochem. Photobiol. A: Chem.* (1995), **6**, 73.
24. Coombes, R; Diggle, A.;Kempcell, S. *Tetrahedron Lett.* (1994), **35**, 6373.
25. Dzengel, J.; Theurich, J.; Bahnemann, D. *Environ. Sci. Technol.* (1999), **33**, 294.

26. Vione, D.; Maurino, V.; Minero, C.; Vincenti, M; Pelizzetti, E. *Chemosphere*. (2001), **44**, 237.
27. Guillame, D.; Morvan, J.; Martin, G. *Environ. Technol. Lett.* (1989), **10**, 491.
28. Beitz, T.; Bechmann, W.; Mitzer, R. *Chemosphere*. (1999) **38**, 351.
29. Eberhardt, M. *J. Phys. Chem.* (1975), **79**, 1067.
30. Montemartini, D. *Acc. Lincei. Roma [IV]*, (1890), **6**, 263.
31. Belson, D.; Strachan, A. *J. Chem. Soc. Perkin Trans. II*, (1989), 15.
32. Veibel, S. *Ber. Dtsch. Chem. Ges.*, (1930), **63**, 1577.
33. Challis, B. C.; Lawson, A. J. *J. Chem. Soc.*, (1971), **1971B**, 770.
34. Pires, M.; Rossi, M. J.; Ross, D. S. *Int. J. Chem. Kinet.*, (1994), **26**, 1207.
35. ChemFinder.com; www.chemfinder.com
36. Handbook of Chemistry and Physics, CRC Press, 1996-1997, 77th Ed.
37. "Infrared Spectroscopy",
<http://www.wpi.edu/Academics/Depts/Chemistry/Courses/CH2670/infrared.html>
38. Mongar, K.; Miller, G. C.; *Chemosphere*, (1988), **17**, 2183.
39. "The Earth's Atmosphere", <http://csep10.phys.utk.edu/astr161/lect/earth/atmosphere.html>.
40. "Ozone Absorption Cross Section", <http://www.aber.ac.uk/ozone/UFAM/o3x-sec.html>
41. "Introduction to Upper Atmospheric Science"
<http://spacescience.nrl.navy.mil/introupatmsci.html>
42. "Light", <http://dosxx.colorado.edu/~bagenal/1010/SESSIONS/13.Light.html>

Figure 1: The Layers of the Atmosphere³⁹

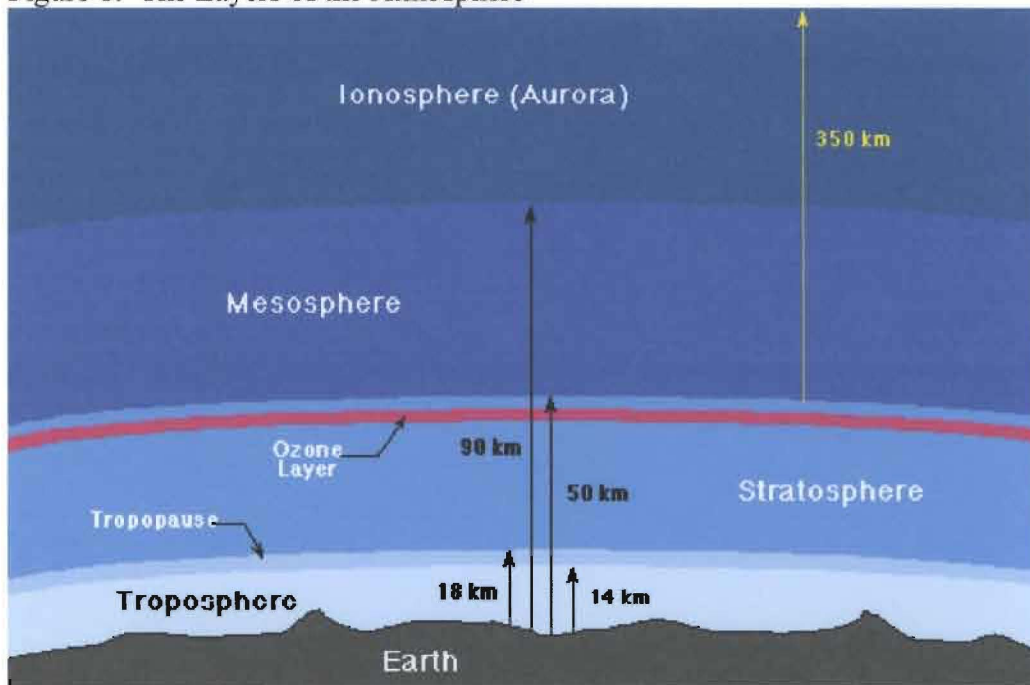


Figure 3: Ozone Absorption Spectrum⁴⁰

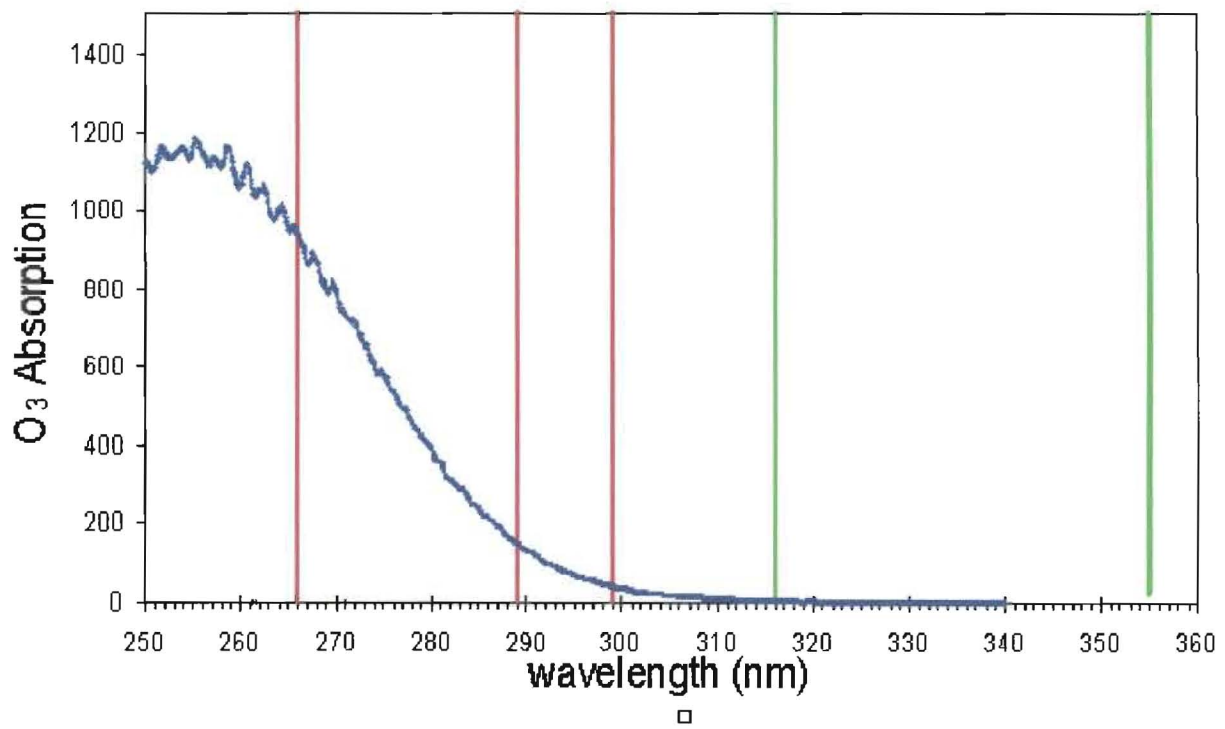
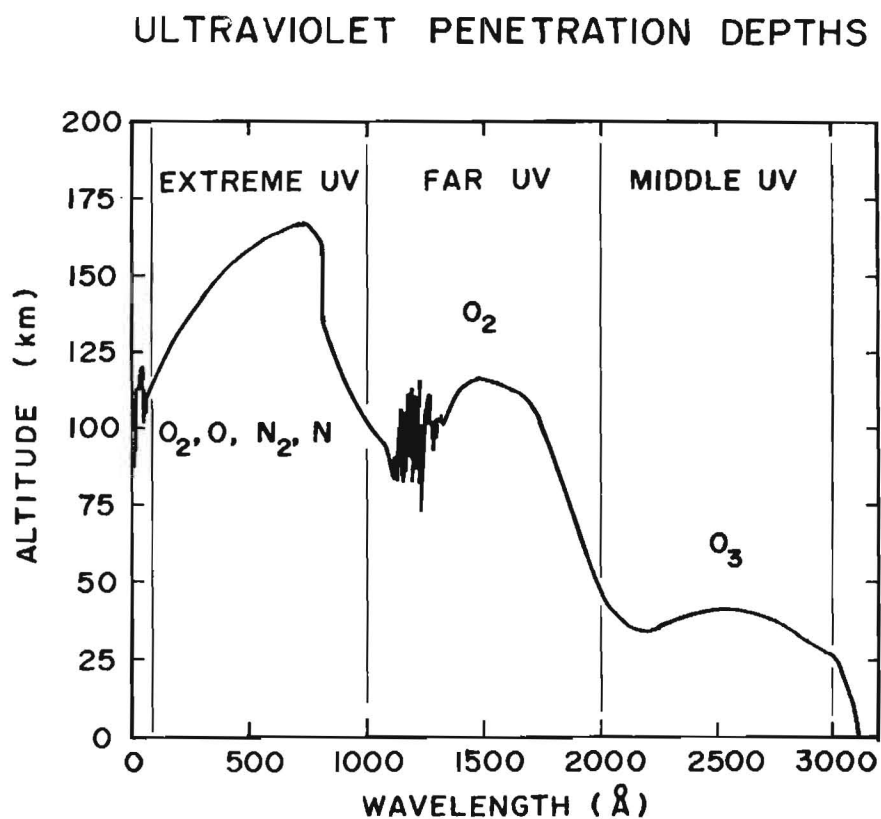


Figure 4⁴¹:



Depths in the Earth's atmosphere, to which half of the vertically incoming ultraviolet radiation (from the Sun or other extraterrestrial source) can penetrate, versus wavelength.

Figure 5⁴²:

THE SOLAR SPECTRUM AT EARTH

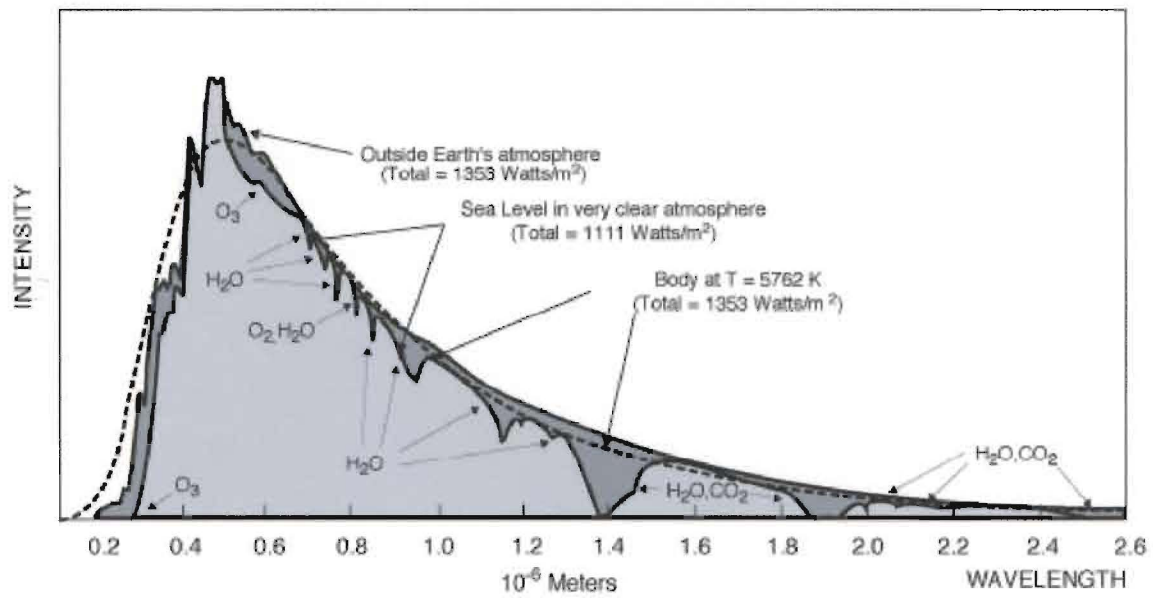


Figure 6: UV-VIS Spectra of NaNO₂ and HONO

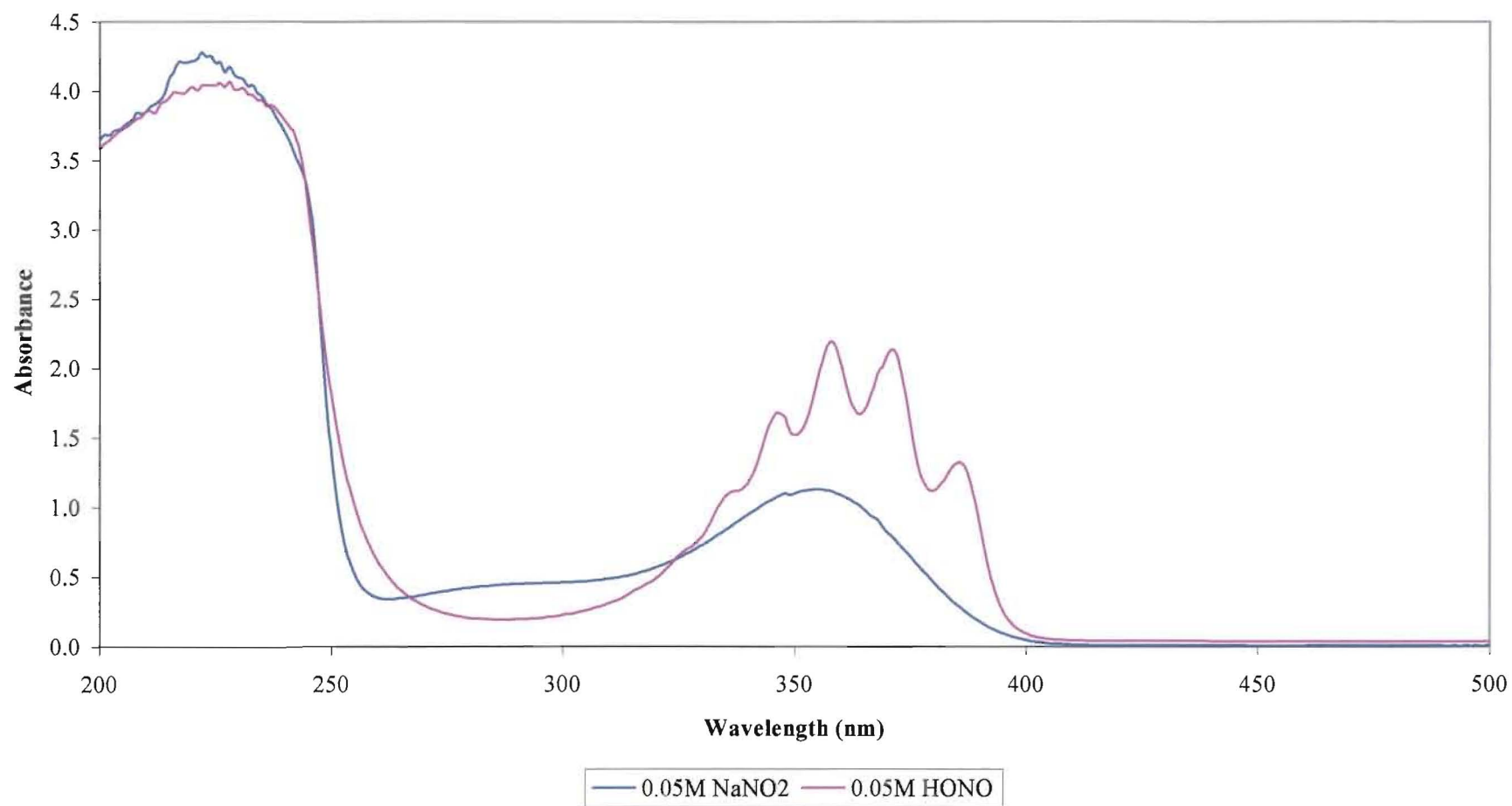


Figure 7: UV-VIS Spectra of Water Saturated with Benzene and 0.05M NaNO₃

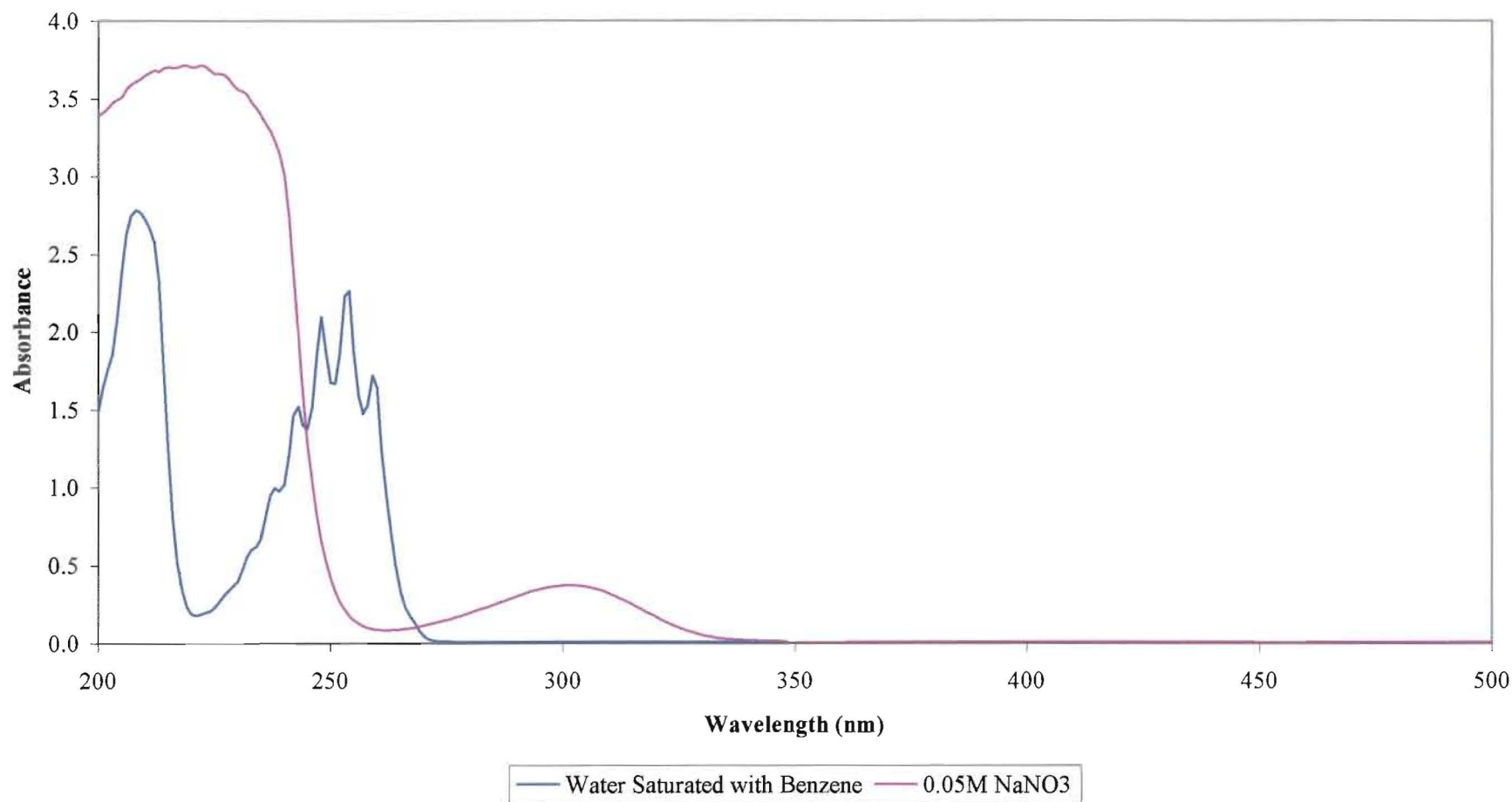


Figure 8: Thermolysis of HONO at -2.0°C

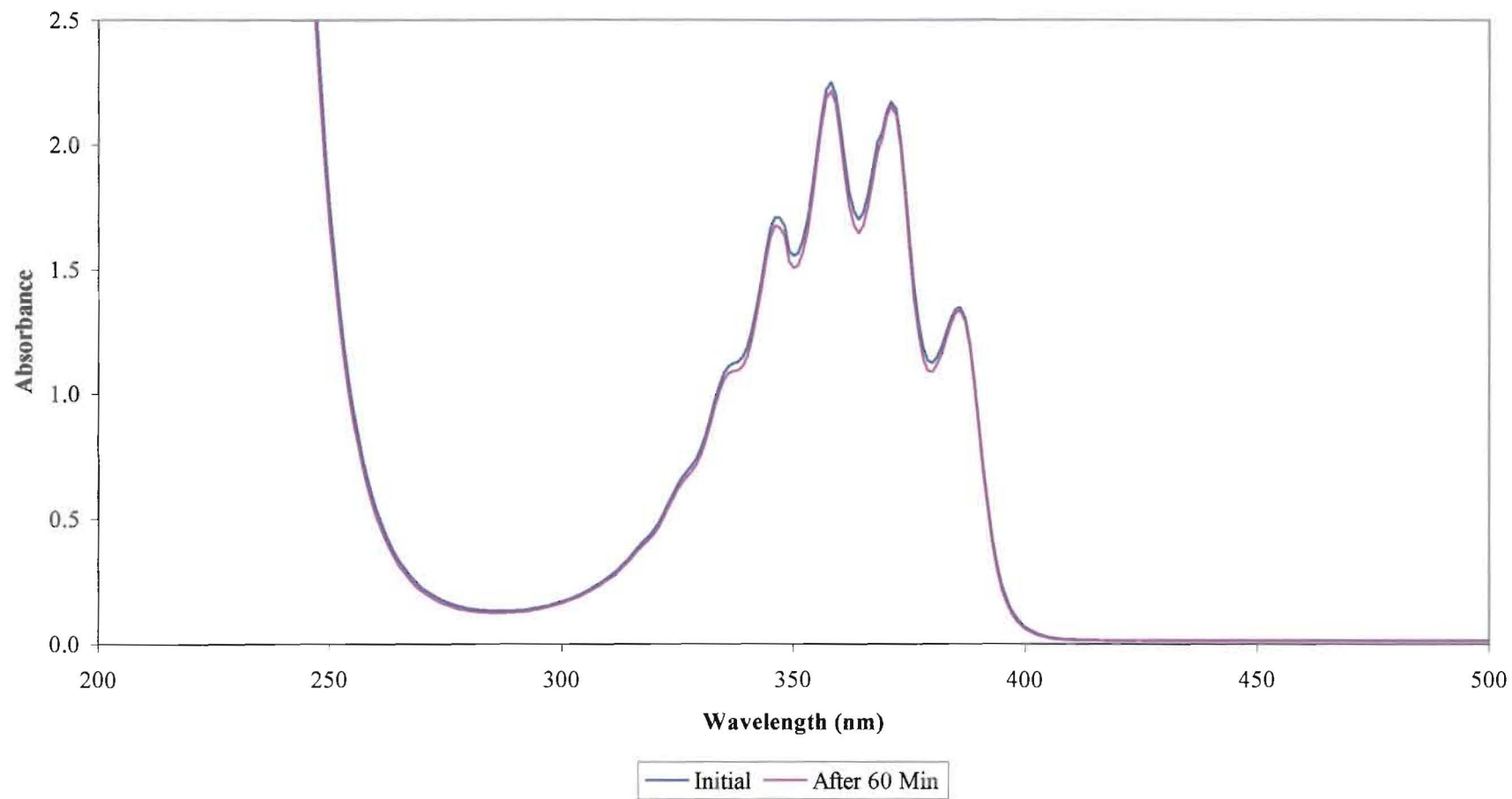


Figure 9: Photolysis of HONO at -2.0°C

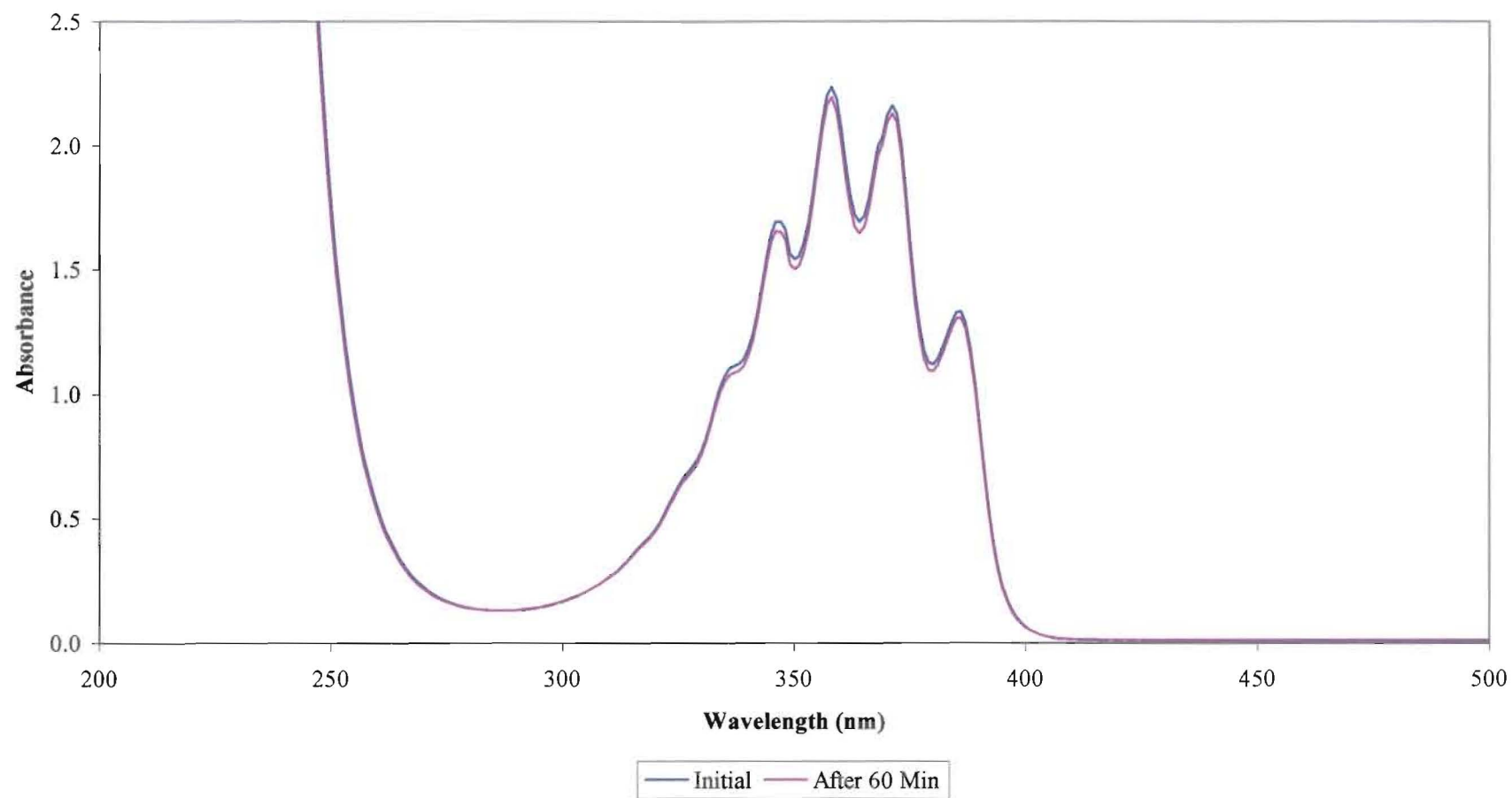


Figure 10: Thermolysis of HONO and Benzene at 2.0°C

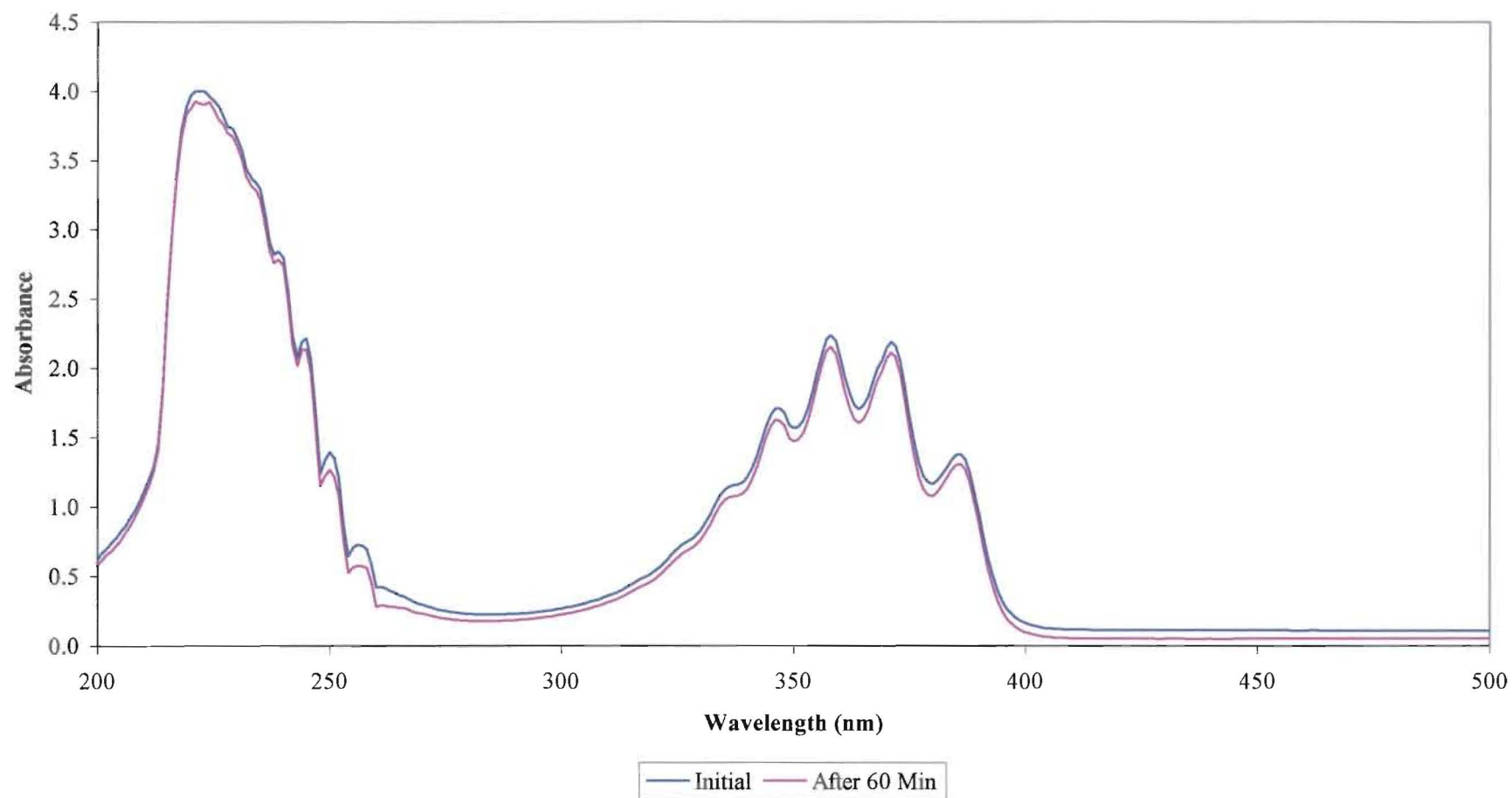


Figure 11: Photolysis of HONO and Benzene at -2.0°C

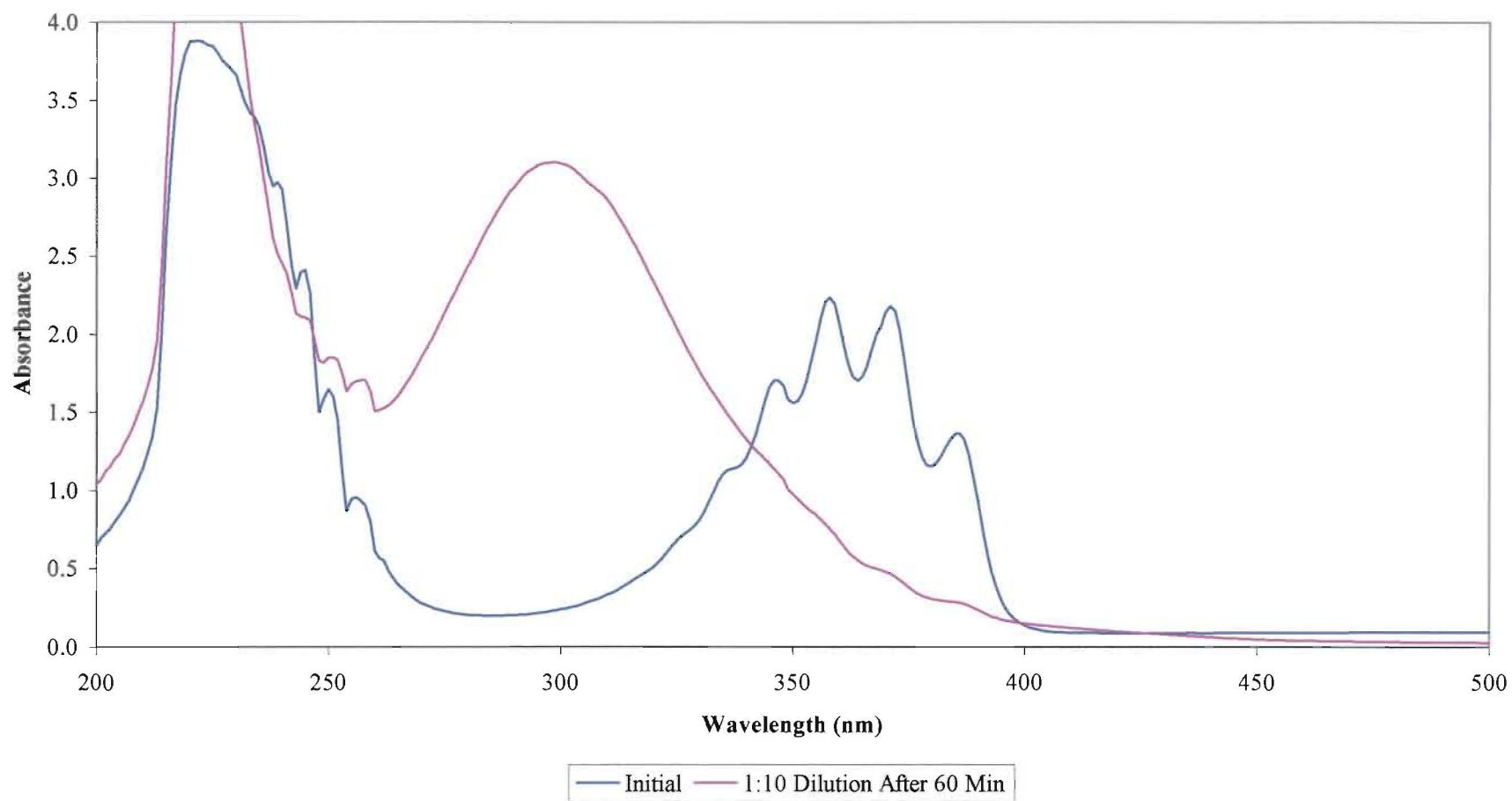


Figure 12: GC-MS of Photolysis Products
TIC: 03012301.D

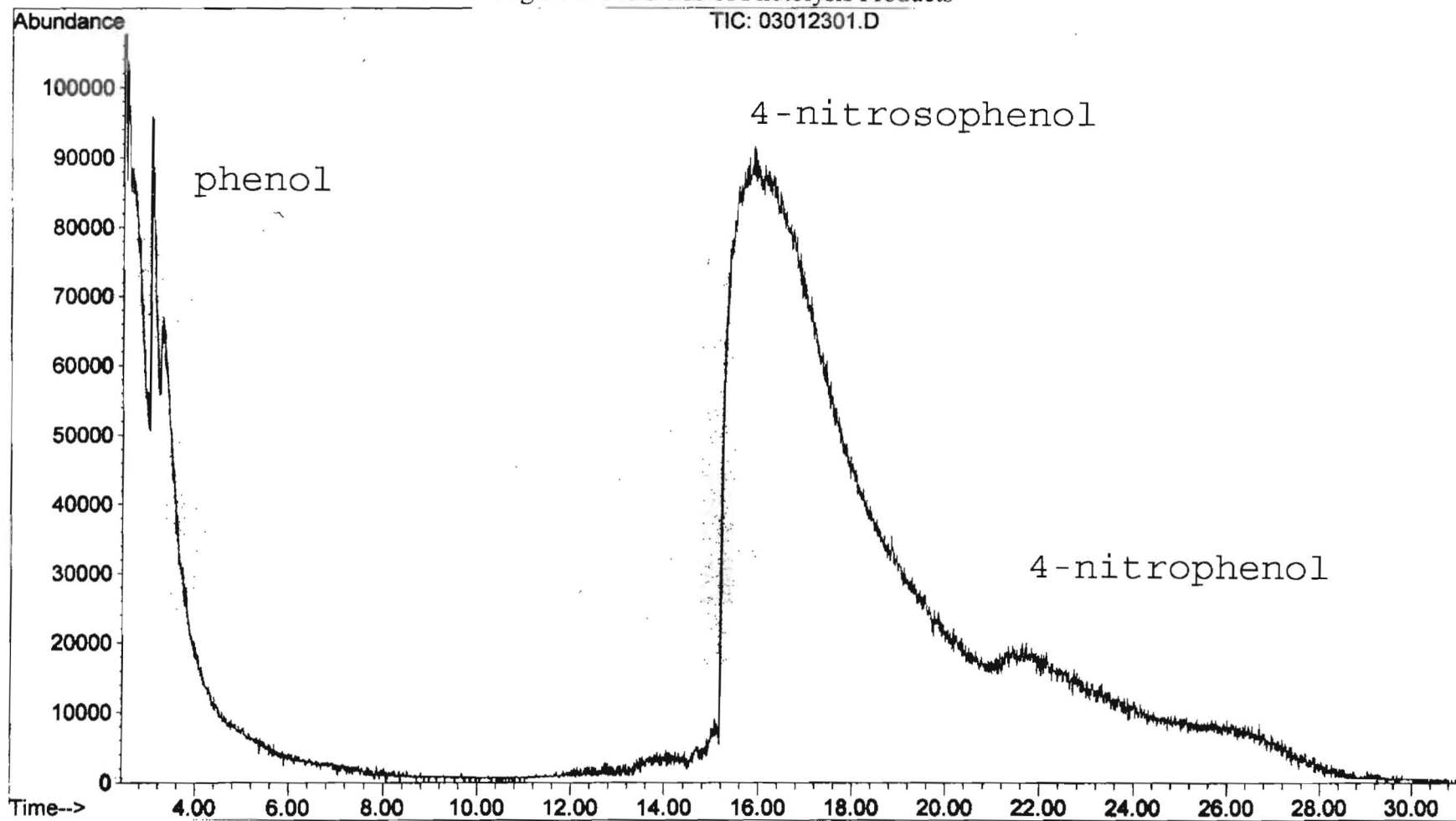


Figure 13: GC-MS of N₂ Purged Photolysis Products

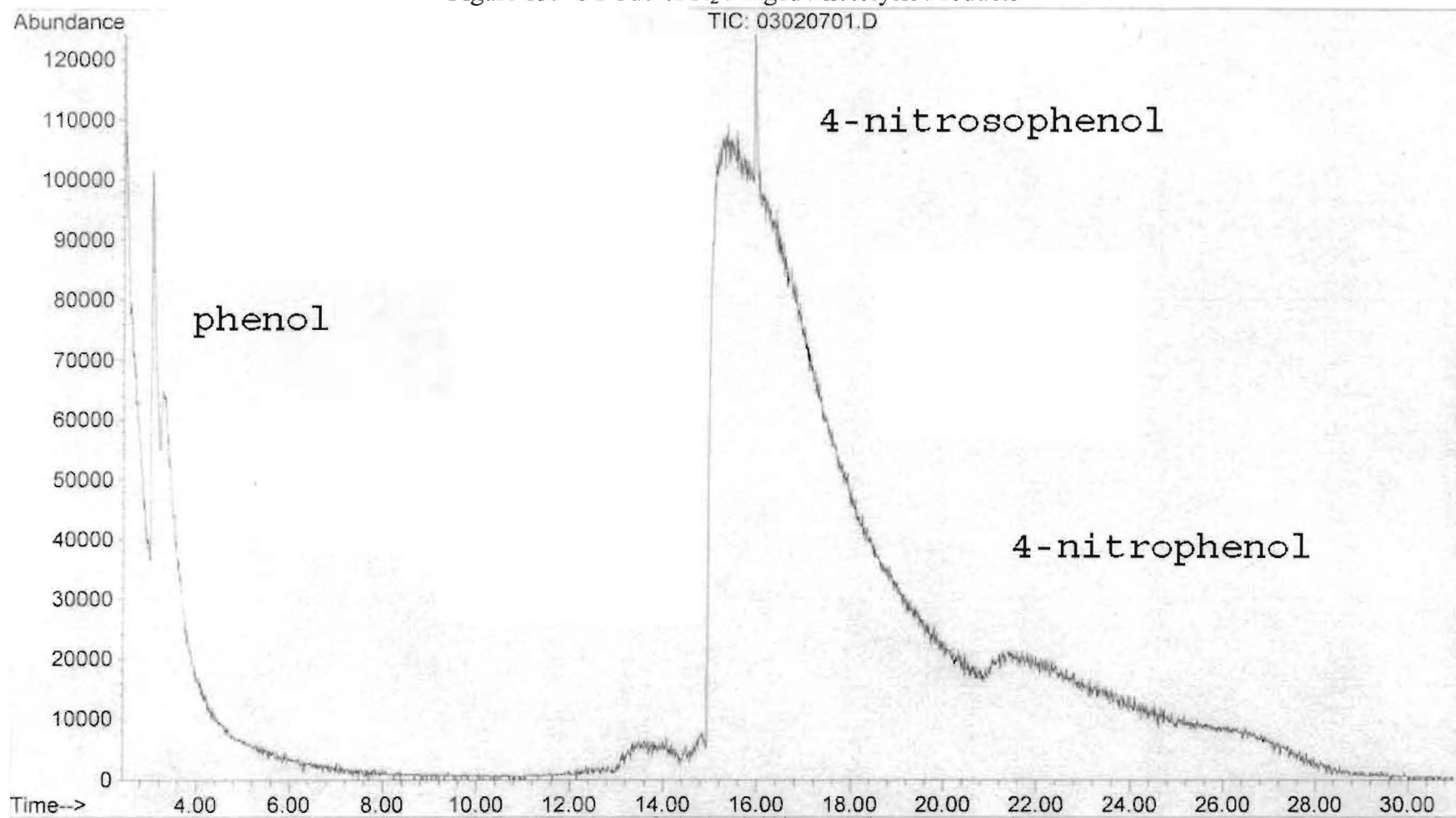


Figure 14: GC-MS of O₂ Purged Photolysis Products

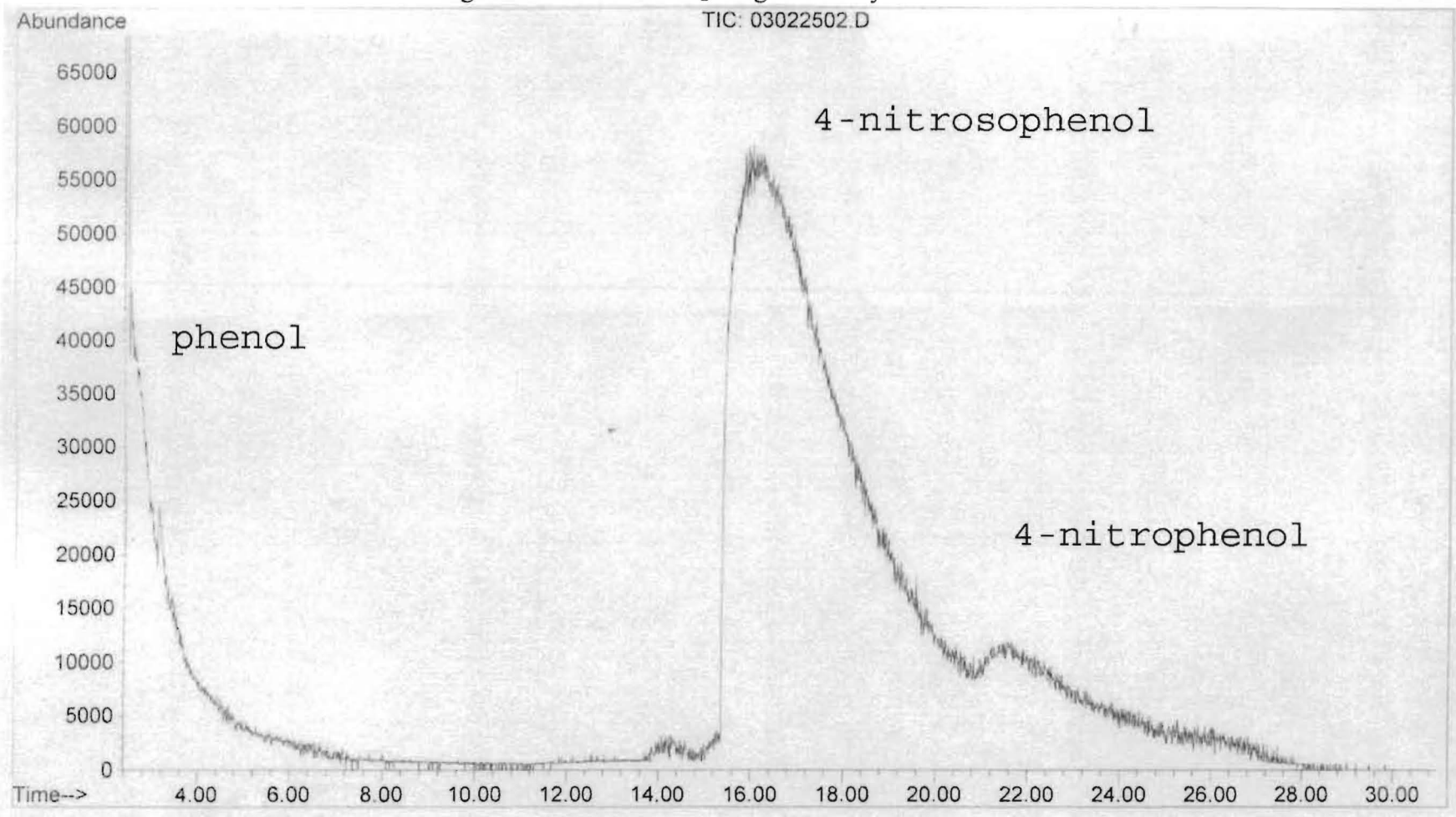


Figure 15: GC-MS of Photolysis Products after 24h

TIC: 03022701.D

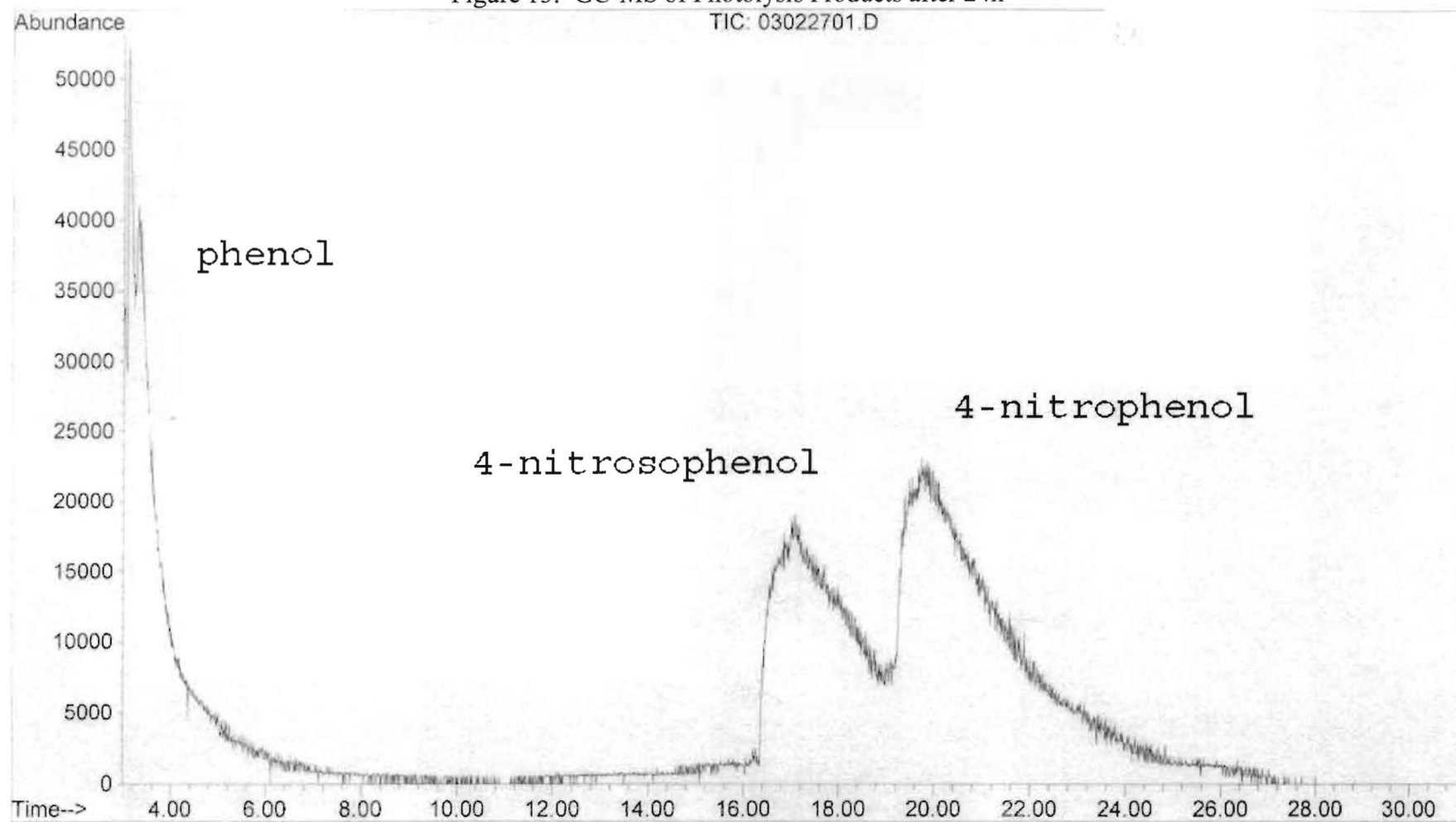


Figure 16: IR of Photolysis Products

